

# Magnetic and lattice excitations in the quasi-2D quantum spin compound (CuCl)LaNb<sub>2</sub>O<sub>7</sub>

Vladimir Gnezdilov<sup>1,2</sup>, Peter Lemmens<sup>1,3</sup>, Dirk Wulferding<sup>4</sup>, Atsushi Kitada<sup>5</sup>, and Hiroshi Kageyama<sup>6</sup>

<sup>1</sup>*Institute for Condensed Matter Physics, TU Braunschweig, Braunschweig D-38106, Germany*

<sup>2</sup>*B. Verkin Institute for Low Temperature Physics and Engineering of the National Academy of Sciences of Ukraine Kharkiv 61103, Ukraine*

E-mail: gnezdilov@ilt.kharkov.ua

<sup>3</sup>*Laboratory of Emerging Nanometrology LENA, Braunschweig D-38106, Germany*

<sup>4</sup>*CCES, Inst. for Basic Science, Dept. Physics and Astronomy, Seoul Nat. Univ., Seoul 08826, Republic of Korea*

<sup>5</sup>*Department of Materials Engineering, Graduate School of Engineering, Kyoto University, Kyoto 615-8510, Japan*

<sup>6</sup>*Department of Energy and Hydrocarbon Chemistry, Graduate School of Engineering, Kyoto University, Kyoto 615-8510, Japan*

Received June 29, 2021, published online September 24, 2021

Raman scattering phonon data of the quasi-two-dimensional quantum spin system (CuCl)LaNb<sub>2</sub>O<sub>7</sub> are used to derive an effective structural model that may serve as a basis for its unconventional magnetic properties. Furthermore, a rich spectrum of magnetic excitations is observed, including quasielastic energy density fluctuations and finite energy bound states. These modes are the key to understand (CuCl)LaNb<sub>2</sub>O<sub>7</sub> as a system with strong interactions between well-localized triplet excitations based on a pronounced competition of magnetic exchange.

Keywords: quantum spin system, Raman scattering, magnetic and lattice excitations.

## 1. Introduction

Low-dimensional quantum spin systems with a spin gap and a quantum disordered singlet ground state are model systems to better understand the relation between topology and the effect of electronic correlations [1, 2]. Many fundamental problems in this field are related to the nature of the ground states, the magnetic excitation spectrum, and the stability of quantum phases without long-range order [3]. These phenomena are most extensively studied for one-dimensional (1D) spin systems like dimerized or frustrated  $S = 1/2$  Heisenberg spin chains, spin ladders and the  $S = 1$  Haldane spin chain. With respect to spin topology, the existence of a singlet ground state in two-dimensional (2D) spin systems is of special interest. Two-dimensionality can be achieved by sufficient physical separation of magnetic layers. Starting from the pioneering work of Wiley *et al.* [4], new low-temperature topotactic strategies, namely intercalation/deintercalation, have allowed designing and constructing new 2D magnetic materials. Among them, the family of compounds (CuX)A<sub>*n*-1</sub>B<sub>*n*</sub>O<sub>3*n*+1</sub> [X = Cl, Br; A is an alkaline earth or rare-earth metal (Ca, Sr, La, ...); B is

a  $d^0$  transition metal (Ti, Nb, Ta, ...)] has attracted particular attention as a two-dimensional quantum spin prototype with frustrated magnetic interactions [5–11].

The subject of our research is the compound (CuCl)LaNb<sub>2</sub>O<sub>7</sub> [4, 5] that belongs to a new class of 2D Heisenberg spin systems with antiferromagnetic (AFM) correlations, a spin-singlet ground state and a finite energy gap (2.3 meV). The underlying magnetic model system might be described by a frustrated square lattice without evidence for a low-temperature 3D magnetic ordering (quantum spin-liquid state). It was shown also that the pure  $J_1$ – $J_2$  model does not describe (CuCl)LaNb<sub>2</sub>O<sub>7</sub> properly and most likely the isolated dimer model with the dimer size of four fourth-nearest-neighbor (4NN) bonds is applicable. Considerable experimental and theoretical efforts have been made to clarify the structural and magnetic properties of this compound [6–22]. However, disagreement remains, and the main one concerns a relevant low-energy spin model. In the research of Tassel *et al.* [18], (CuCl)LaNb<sub>2</sub>O<sub>7</sub> was identified as a Shastry–Sutherland system with ferromagnetic interdimer couplings. At the same time, Tsirlin *et al.* [17] established (CuCl)LaNb<sub>2</sub>O<sub>7</sub> as a nonfrustrated system

of coupled spin dimers with predominant antiferromagnetic interactions. Therefore, additional spectroscopic data are needed.

Raman spectroscopy is a complimentary tool for such systems study as it can provide valuable information about spin and lattice degrees of freedom and their mutual coupling. It is especially sensitive to fluctuations and multi-particle effects [23, 24]. Unfortunately, to our knowledge, there exist no Raman scattering study of the  $(\text{CuX})\text{A}_{n-1}\text{B}_n\text{O}_{3n+1}$  system. Therefore, in this paper, we present related data including a comparison with  $(\text{CuBr})\text{LaNb}_2\text{O}_7$  playing special emphasis on a discussion of the magnetic excitation spectrum. We observed several distinct features: (i) anomalous temperature behavior of phonon excitations, indicating strong spin-phonon coupling; (ii) exotic temperature behavior of magnetic quasielastic light scattering, indicating the presence of quantum fluctuations down to the lowest temperature of the experiment; (iii) single triplet mode, well-defined bound state modes at temperatures  $T \ll \Delta$ , and two-magnon signal contributing to spectra up to higher temperatures.

Our results provide experimental evidence of the frustrated magnetic interactions that are inherent to the Shastry–Sutherland model, and therefore support the conclusions of the Ref. 18 defining  $(\text{CuCl})\text{LaNb}_2\text{O}_7$  as ferromagnetically coupled Shastry–Sutherland-type quantum spin system.

## 2. Experimental

The studied layered perovskite oxide  $(\text{CuCl})\text{LaNb}_2\text{O}_7$  has been prepared from low-temperature ion-exchange reaction [5]. An Ar/Kr ion laser was used for Raman excitation at 514.5 nm (2.41 eV). The laser output power was kept below 3 mW on a focus of approximately 50  $\mu\text{m}$  diameter to protect the sample from possible heating effects. The scattered light was collected in quasi-backscattering configuration and dispersed by a triple monochromator DILOR XY on a liquid-nitrogen-cooled CCD detector (Horiba Jobin Yvon, Spectrum One CCD-3000V) with a spectral resolution of  $< 0.5 \text{ cm}^{-1}$ . Temperature-dependent Raman spectra were measured in a continuous helium flow optical cryostat by varying temperature from 1.5 K to room temperature. Measurements on polycrystalline samples were performed with vertical polarization of the incident laser light. Polarization of the scattered light was not analyzed.

## 3. Results and discussion

### 3.1. Crystal structure and phonon spectra

Initially, the crystal structure of  $(\text{CuCl})\text{LaNb}_2\text{O}_7$  (Fig. 1) was refined in the tetragonal space group  $P4/mmm$  (No. 123,  $Z = 1$ ) with magnetic CuCl sheets widely separated by nonmagnetic  $\text{Nb}_2\text{O}_7$  double-perovskite slabs [4]. In this structure, Cl ions are located in the special  $1b$  posi-

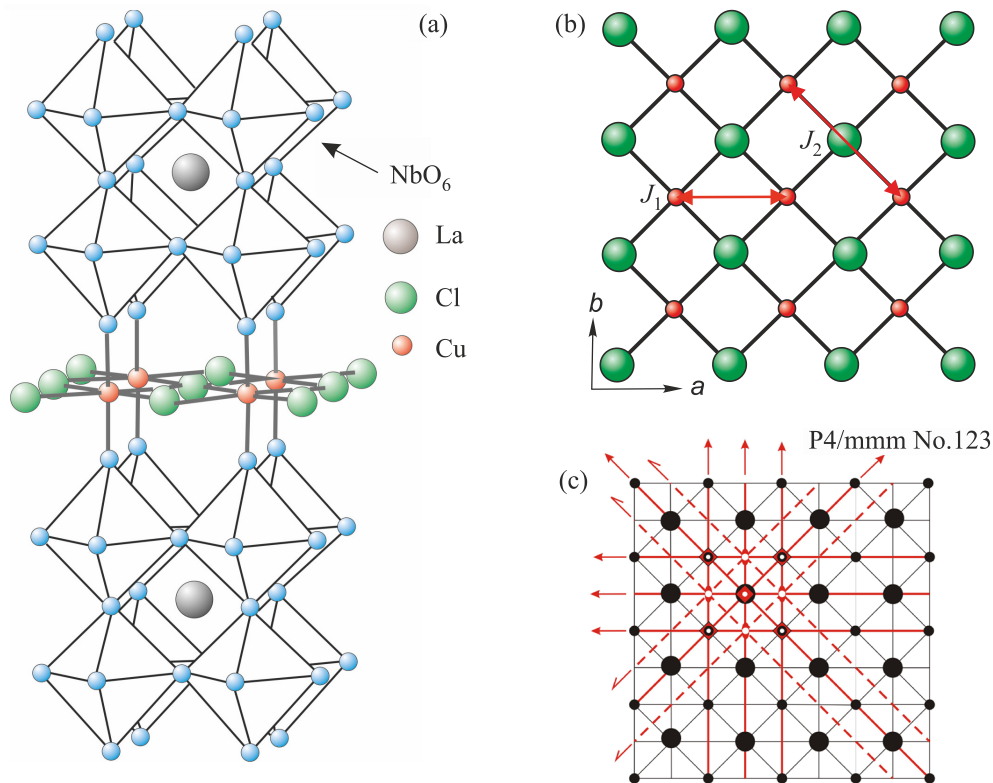


Fig. 1. (Color online) (a) Crystal structure of  $(\text{CuCl})\text{LaNb}_2\text{O}_7$ . (b) Exchange interactions  $J_1$  and  $J_2$  on the 2D square lattice. (c)  $P4/mmm$  structure and symmetry elements for the  $\text{CuCl}$  plane of  $(\text{CuCl})\text{LaNb}_2\text{O}_7$ . Bigger and smaller circles represent the Cl and Cu ions, respectively.

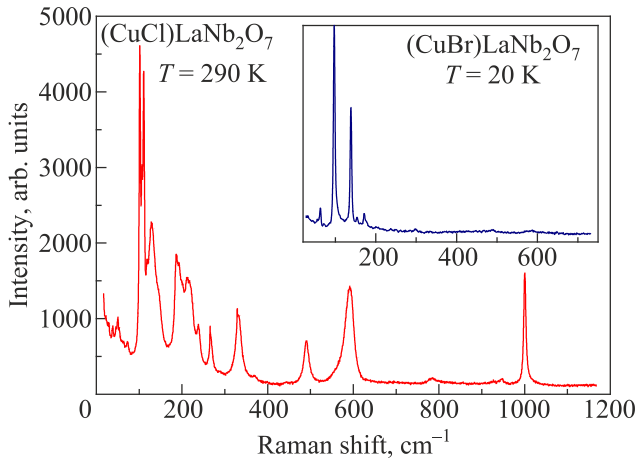


Fig. 2. Raman spectrum of (CuCl)LaNb<sub>2</sub>O<sub>7</sub> at room temperature. The inset shows the spectrum of the sister compound (CuBr)LaNb<sub>2</sub>O<sub>7</sub> at  $T = 20$  K.

tions  $(0, 0, 1/2)$  and copper ions have a squeezed octahedral coordination with four equal Cu–Cl bonds [ $d(\text{Cu–Cl}) = 2.74 \text{ \AA}$ ], see Figs. 1(a) and 1(b). Based on this, a Heisenberg spin model with the nearest-neighbor exchange  $J_1$  and the second nearest-neighbor exchange  $J_2$  [the so-called  $J_1$ – $J_2$  model, see Fig. 1(b)] has been considered as appropriate. More realistic structural modelling discussed in Ref. 25 considers the same  $P4/mmm$  structure, but with the Cl atoms randomly occupying one quarter of  $4m$  sites  $(x, 0, 1/2)$  with  $x = 0.136$ . This model yields two short and two long Cu–Cl bonds. The information obtained from all subsequent experiments has raised serious doubt against the validity of the initially proposed  $J_1$ – $J_2$  model. Considering that precise structural information of the CuCl plane is crucial to understand the origin of the (CuCl)LaNb<sub>2</sub>O<sub>7</sub> physics, let's first analyze our Raman data in comparison with the available structural information.

A room temperature Raman spectrum of (CuCl)LaNb<sub>2</sub>O<sub>7</sub> is presented in Fig. 2. The sharpness of the observed phonon modes indicates the high quality of our sample. Experimentally, 29 phonon modes are identified in the frequency region of 16–1170  $\text{cm}^{-1}$ .

For the tetragonal  $P4/mmm$  (No. 123,  $Z = 1$ ) crystal structure of (CuX)LaNb<sub>2</sub>O<sub>7</sub> ( $X = \text{Cl}, \text{Br}$ ), only 8 Raman active phonon modes ( $\Gamma_{\text{Raman}} = 3A_{1g} + B_{1g} + 4E_g$ ) are allowed. Such a tetragonal structure with a square CuCl lattice of (CuCl)LaNb<sub>2</sub>O<sub>7</sub> is inconsistent with our observations, since at room temperature we observe a significantly larger number of phonon lines in the Raman spectra. At the same time, in the Raman spectra of the sister compound (CuBr)LaNb<sub>2</sub>O<sub>7</sub> (see inset in Fig. 2) we can surely identify only 8 phonon lines (even if there are additional lines in the low-temperature spectra, their intensity is negligible). This indicates that the distortions from the ideal  $P4/mmm$  structure in (CuBr)LaNb<sub>2</sub>O<sub>7</sub> are much smaller than in (CuCl)LaNb<sub>2</sub>O<sub>7</sub>.

The structure of (CuCl)LaNb<sub>2</sub>O<sub>7</sub> was analyzed by means of nuclear magnetic resonance (NMR), nuclear quadrupole

resonance (NQR), and transmission electron microscopy (TEM) measurements [8]. NQR spectra evidenced a lack of tetragonal symmetry and revealed single sites of Cu, Cl, and La atoms, hence suggesting the ordering of the Cl atoms, at least on a local scale. TEM measurements revealed weak reflections in addition to strong fundamental reflections relevant to the earlier reported tetragonal crystal structure. The weak reflections are commensurate and indicate the doubling of the lattice period of both  $a$  and  $b$  axes. Such a superstructure has not been detected by high-resolution synchrotron x-ray diffraction [9], and the specific ordering pattern remains unclear.

Assuming that a big enough spin-gap in (CuCl)LaNb<sub>2</sub>O<sub>7</sub> can be caused by the formation of Cu dimers, different variants of structure (Fig. 3) have been proposed in Ref. 8. In all these structures, Cu maintains the ideal position for the square lattice  $(1/2, 1/2, 1/2)$ . The structure in Fig. 3(a) is simplest and has only one Cu and Cl site. The factor group analysis yields 33 Raman-active phonon modes ( $\Gamma_{\text{Raman}} = 10A_g + 7B_{1g} + 7B_{2g} + 9B_{3g}$ ) for this orthorhombic  $Cmmm$  (No. 65,  $Z = 2$ ) structure. The latter result is quite close to the Raman experiment, however, the unit vector of the structure 3(a) leads to a superstructure reflection at  $(1/2, 1/2, 0)$  but cannot account for the TEM observed reflections such as  $(1/2, 0, 0)$  and  $(0, 1/2, 0)$  [8].

Three other models, consistent with both MQR and TEM results, were also considered in Refs. 8 and 10. Figures 3(b), 3(c), and 3(d) show examples of such structures with Cl in more general positions. In the structure 3(b), Cl moves off the ideal  $(0, 0, 1/2)$  position to a position  $(x, y, 1/2)$ ,  $(-x, y, 1/2)$ ,  $(x, -y, 1/2)$ , or  $(-x, -y, 1/2)$ . In the structures 3(c) and 3(d) Cl moves off to  $(x, 0, 1/2 + \delta)$ ,  $(x, 0, 1/2 - \delta)$ ,  $(-x, 0, 1/2 + \delta)$ , or  $(-x, 0, 1/2 - \delta)$ . Structures 3(c) and 3(d) have the same exchange paths which differ from the exchange paths of the structure 3(b). All models 3(b), 3(c), and 3(d) generate frustration. The factor group analysis yields 66 Raman-active phonon modes for the orthorhombic  $Pbam$  (No. 55,  $Z = 4$ ) 3(b) structure, and 64 and 60 Raman-active phonon modes for the orthorhombic  $Pmmm$  (No. 59,  $Z = 4$ ) 3(c) and  $Pmna$  (No. 53,  $Z = 4$ ) 3(d) structures, respectively. So, these structures are inconsistent with our room temperature Raman scattering data. Here we note that the atomic structure of (CuX)LaNb<sub>2</sub>O<sub>7</sub> ( $X = \text{Cl}, \text{Br}$ ) was investigated in Ref. 15 using the density functional calculations including relaxation. The authors concluded that both compounds have orthorhombic  $Pbam$  structure as proposed by Yoshida *et al.* [8, 10].

The structural distortion of the Cl-atom position means that, in the CuClO<sub>2</sub> layers of (CuCl)LaNb<sub>2</sub>O<sub>7</sub>, the CuCl<sub>4</sub>O<sub>2</sub> octahedra with two short Cu–Cl<sub>s</sub> and two long Cu–Cl<sub>l</sub> bonds are realized. When all the CuCl<sub>4</sub>O<sub>2</sub> octahedra have the four-short-two-long coordination with linear Cl<sub>s</sub>–Cu–Cl<sub>s</sub> units, the CuClO<sub>2</sub> layer is divided into CuClO<sub>2</sub> chains of corner-sharing CuCl<sub>2</sub>O<sub>2</sub> rhombuses. There are two reports that consider such type of Cl-ions arrangement [12, 13]. In the paper of Whangbo and Dai [12], only one leading an-

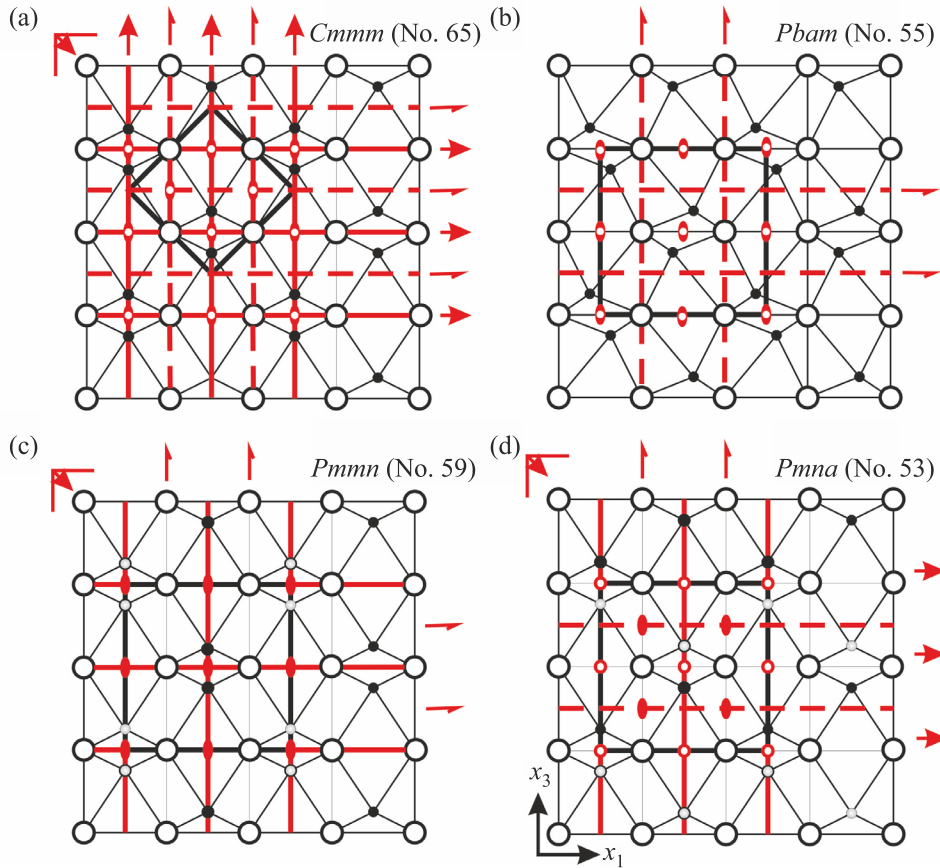


Fig. 3. (Color online) Possible structures and symmetry elements for the CuCl plane of  $(\text{CuCl})\text{LaNb}_2\text{O}_7$ . Bigger and smaller circles represent Cl and Cu ions, respectively. The solid thick lines in (a), (b), (c), and (d) indicate the unit cell. In the structures (c) and (d) open and grey-filled spheres represent the Cl atoms above and below the Cu plane, respectively. Copper is assumed to remain in ideal positions for the square lattice  $(1/2, 1/2, 1/2)$ .

tiferromagnetic coupling  $J_1$  was considered. These authors could not confirm the existence of a spin-gap behavior and, finally, discarded such a model. In a computational study of the  $(\text{CuCl})\text{LaNb}_2\text{O}_7$  [13], numerous inequivalent exchange couplings in the distorted CuCl layer were taken into account. It was concluded that the lack of the tetragonal symmetry and long-range interactions lead to a complex spin model with chains running in the CuCl plane and sizable inter-

chain couplings. The in-plane interchain interactions are frustrated and may account for the spin-gap behavior.

An outstanding model for CuCl layers arrangement with four long and two short Cu–Cl bonds [orthorhombic  $Pmma$  (No. 51,  $Z = 2$ ) structure, see Fig. 4] was proposed in Ref. 12. For this orthorhombic structure, 30 Raman-active phonon modes are allowed. This value looks very close to our Raman experiment. The resulting spin lattice

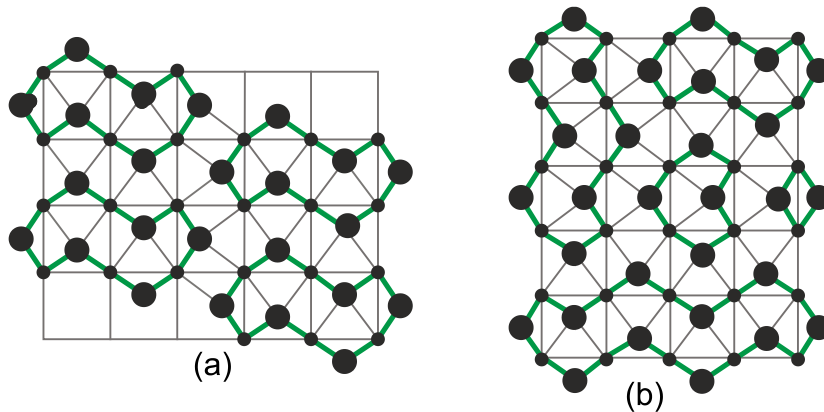


Fig. 4. (Color online) CuCl layers in  $(\text{CuCl})\text{LaNb}_2\text{O}_7$  composed of  $2n$ -ring clusters: (a) with long-range order ( $2n = 6$ ) and (b) without long-range order ( $2n \geq 2$ ) [12]. The short CuCl bonds are shown with thick green lines.

that includes nonlinear Cl<sub>5</sub>–Cu–Cl<sub>5</sub> units does not have uniform spin chains but can be divided into  $2n$ -ring clusters of varying sizes with or without long-range structural order. This model should definitely be considered interpreting the magnetic properties of (CuCl)LaNb<sub>2</sub>O<sub>7</sub> determined by neutron scattering and magnetization experiments. Note that in all the above-mentioned variants of the crystal structure of (CuCl)LaNb<sub>2</sub>O<sub>7</sub> copper remains on the ideal (1/2, 1/2, 1/2) positions.

The most recent single-crystal x-ray diffraction and powder neutron diffraction data [20] allows to further clarify the complex and subtle superstructure occurring in (CuCl)LaNb<sub>2</sub>O<sub>7</sub> within the correct  $2 \times a_t$ ,  $2 \times b_t$ ,  $c_t$  unit-cell of *Pbam*. It is shown that Cu and Cl in the CuCl plane occupy a single independent crystallographic site (exactly at  $z/c = 1/2$ ), namely a  $4h$  Wyckoff position, without disorder. The Cu atom is displaced along the  $y$  direction by 0.13 Å with regard to the ideal (1/2, 3/4, 1/2) position. Therefore, the sublattice of Cu<sup>2+</sup> ions cannot be described by a perfect square lattice. The apical oxygen of the NbO<sub>6</sub> octahedrons is displaced in phase with respect to its bonded Cu in such a way that the angle between Cu–O bond and  $z = 1/2$  plane remains unmodulated and almost equal to 90°. The distortion for the Cl atom is 0.56 Å with respect to the ideal site at (3/4, 1/2, 1/2) with a slight component along  $a$  and a main component along  $b$ . These distortions explain the doubling of the unit-cell along both  $a$  and  $b$  axes. Finally, this structural model is similar to the one proposed by Tsirlin *et al.* [16], except for the choice of the  $a$  and  $b$  pseudo-tetragonal parameters.

Here, a factor group analysis yields 84 Raman-active phonon modes ( $\Gamma_{\text{Raman}} = 21A_g + 21B_{1g} + 21B_{2g} + 21B_{3g}$ ) for the *Pbam* structure of (CuCl)LaNb<sub>2</sub>O<sub>7</sub> with Cu, Cl, La, Nb, O1, O2, O3, O4, and O5 in the  $4h$ ,  $4h$ ,  $4g$ ,  $8i$ ,  $4f$ ,  $4e$ ,  $4g$ , and  $8i$  Wyckoff positions, respectively. However, in our Raman spectrum, even at lowest temperatures, it is impossible to observe more than 38 phonon lines. The big deficit of the observed Raman lines compared to the latter symmetry

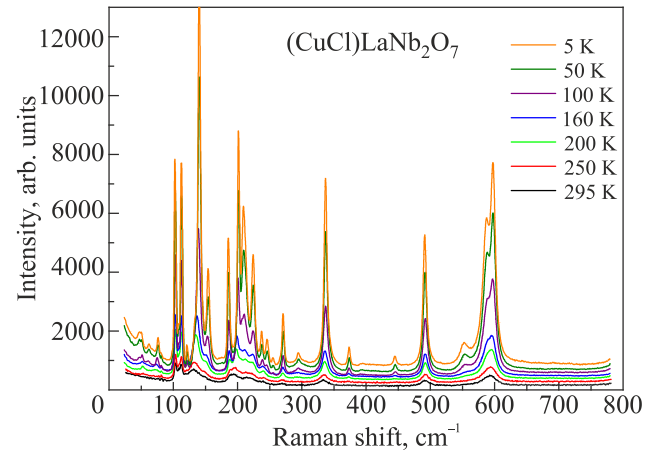


Fig. 5. (Color online) Raman spectra of (CuCl)LaNb<sub>2</sub>O<sub>7</sub> at selected temperatures.

analysis is assigned to rather small deviations of the ions from the ideal positions. Therefore, we propose that on a limited coherence length a simplified model (see, e.g., Ref. 26) with higher symmetry of the complexes is sufficient. Closeness of a real arrangement of some structural units to higher symmetry than the Wyckoff position results in strong inter-ferential quenching of a number of Raman lines in the spectra. A similar approach can be applied to (CuBr)LaNb<sub>2</sub>O<sub>7</sub>, the structure of which was defined as pseudo-tetragonal *Cmmm* [27]. Although the high-resolution x-ray measurements have identified weak orthorhombic distortions, they are obviously so small that in the Raman spectra (Fig. 2) one can confidently identify only 8 phonon modes.

The temperature evolution of the Raman spectra of (CuCl)LaNb<sub>2</sub>O<sub>7</sub> measured in the frequency region of 20–780 cm<sup>-1</sup> at temperatures 5–295 K is shown in Fig. 5.

To get more insight into the phonon dynamics, we analyzed the temperature dependence of the phonon line parameters. Phonon lines were fitted with Lorentzian profiles in the whole investigated temperature range and results are presented in Fig. 6, where the temperature-dependent pa-

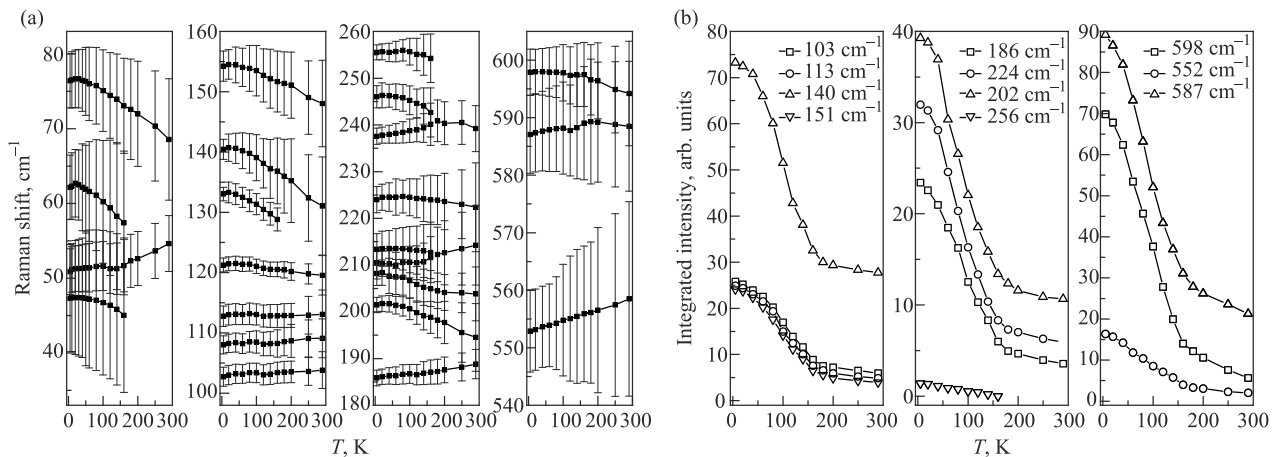


Fig. 6. Temperature dependences of the (a) selected phonon frequencies (bars display the width of phonon lines at half of maximum) and (b) integrated intensities in the Raman spectra of (CuCl)LaNb<sub>2</sub>O<sub>7</sub> measured in the temperature range of 5–295 K.

rameters of representative phonon modes are plotted. Our Raman scattering experiments on  $(\text{CuCl})\text{LaNb}_2\text{O}_7$  show anomalies in the phonon spectra at a characteristic temperature  $T^* \sim 170$  K (Figs. 5 and 6). With decreasing temperatures, additional lines appear with small intensities. Some lines split with frequency separations of a few %. Furthermore, there exist more pronounced intensity anomalies, i.e., there is a step-like intensity gain of many modes for  $T < T^*$ . It is noteworthy that this anomaly cannot be assigned to a specific mode or range of phonon frequencies. Therefore, we cannot assign it to a specific coordination, as it, e.g., would be the case for a specific structural instability.

However, as Raman scattering intensity is related to a polarizability of the involved electronic wave functions, we can discuss a modification of covalency. In a recent review of low-dimensional transition metal compounds with  $p$ -electron ligands [28] and an earlier work of the effect of covalency on the magnetism of spin-chain materials [29], it has been highlighted that such states are prone to instabilities as they suppress magnetic long-range ordering due to enhanced Hunds coupling and ferromagnetic exchange paths that introduce effective competing interactions. Such covalency leads to interplay between crystal structure and magnetic properties that is well known and characteristic for many low-dimensional spin systems. The formation of local dimers for temperatures that are comparable to the largest exchange coupling leads to a crossover regime where phonon anomalies are observed [30–32]. We interpret the observed phonon anomalies in  $(\text{CuCl})\text{LaNb}_2\text{O}_7$  as being related to such a crossover.

### 3.2. Magnetic excitations

The magnetic susceptibility and inelastic neutron scattering data of  $(\text{CuCl})\text{LaNb}_2\text{O}_7$  are typically for antiferromagnetic correlations without evidence for long-range order [5]. Currently, there are two main models describing its spin system [17, 18]. They are both based on spin dimers with relevance of fourth neighbors and relevance of  $\text{Cu}-\text{Cl}-\text{Cl}-\text{Cu}$  exchange paths. For the latter, a deviation from tetragonal symmetry is essential. The difference is that in the Ref. 17  $(\text{CuCl})\text{LaNb}_2\text{O}_7$  was established as a nonfrustrated system of coupled spin dimers with predominant antiferromagnetic interactions while in Ref. 18 it was described by a ferromagnetic version of the Shastry–Sutherland model [33] with inherent magnetic frustration.

Magnetic scattering in  $(\text{CuCl})\text{LaNb}_2\text{O}_7$  is evident as quasi-elastic scattering (QS,  $E \approx 0$ ) and as several distinct finite-energy modes, both with characteristic temperature dependences in intensity and frequency. First, we will discuss the quasi-elastic Raman response shown in Fig. 7(a). Our experimental setup was suitably adjusted so that Rayleigh scattering is suppressed for frequencies above  $\omega > 12$   $\text{cm}^{-1}$ , and therefore the observed scattering is intrinsic. Such a quasi-elastic scattering contribution with Lorentzian lineshape is attributed to fluctuations of the energy density of the spin

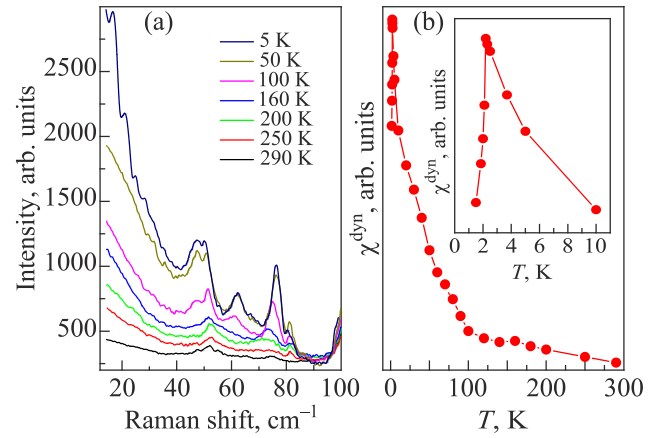


Fig. 7. (Color online) (a) Quasielastic light scattering in  $(\text{CuCl})\text{LaNb}_2\text{O}_7$  at selected temperatures. (b) Temperature dependence of the dynamic spin susceptibility  $\chi^{\text{dyn}}$ . Inset shows low-temperature part of the  $\chi^{\text{dyn}}(T)$ .

system [34, 35]. In contrast, a Gaussian lineshape would point to diffusive dynamics [36, 37]. There are several studies of energy density fluctuations [34, 35] with Gaussian lineshape [38].

Quasielastic light scattering intensity in  $(\text{CuCl})\text{LaNb}_2\text{O}_7$  shows a pronounced temperature dependence — its intensity increases with decreasing temperature. This indicates the enhancement of spin fluctuations upon cooling. To further understand its temperature evolution, we have evaluated the dynamic spin susceptibility  $\chi^{\text{dyn}}$ , similar to Refs. 39, 40, using the Kramer–Kronig relation [41]

$$\chi^{\text{dyn}} \equiv \frac{2}{\pi} \int_0^{\infty} \frac{\chi''(\omega)}{\omega} d\omega.$$

This is done as follows. First we derive Raman conductivity  $\chi''/\omega$ , where  $\chi''$  is the Raman response obtained from the raw quasi-elastic intensity, by dividing it by the Bose thermal factor. Then we extrapolate  $\chi''/\omega$  till 0  $\text{cm}^{-1}$  and, after subtracting the phonon response, integrate up to the upper threshold value of energy where  $\chi/\omega$  does not further change. Figure 7(b) shows the temperature evolution of  $\chi^{\text{dyn}}$ . With decreasing temperature from 290 K,  $\chi^{\text{dyn}}$  shows a weak temperature dependence, reaching a plateau at approximately  $\sim 100$ – $150$  K. With further cooling, there is an increase with larger slope. At lowest temperature, there is a sharp drop for  $T < 2.2$  K, see inset. For a paramagnetic phase with uncorrelated spins,  $\chi^{\text{dyn}}$  should be temperature independent. Instead, the observed temperature dependence of  $\chi^{\text{dyn}}$  signals a crossover to a proximate quantum spin liquid with cooling to  $T \approx 120$  K. The further increasing  $\chi^{\text{dyn}}$  in the temperature range from  $\sim 120$  to 2.2 K indicates the strong growth of dynamic quantum fluctuations associated with spin degree of freedom. The sudden sharp decrease in  $\chi^{\text{dyn}}$  with cooling below 2.2 K could be associated with the onset of spin freezing. However, systems with fractionalized

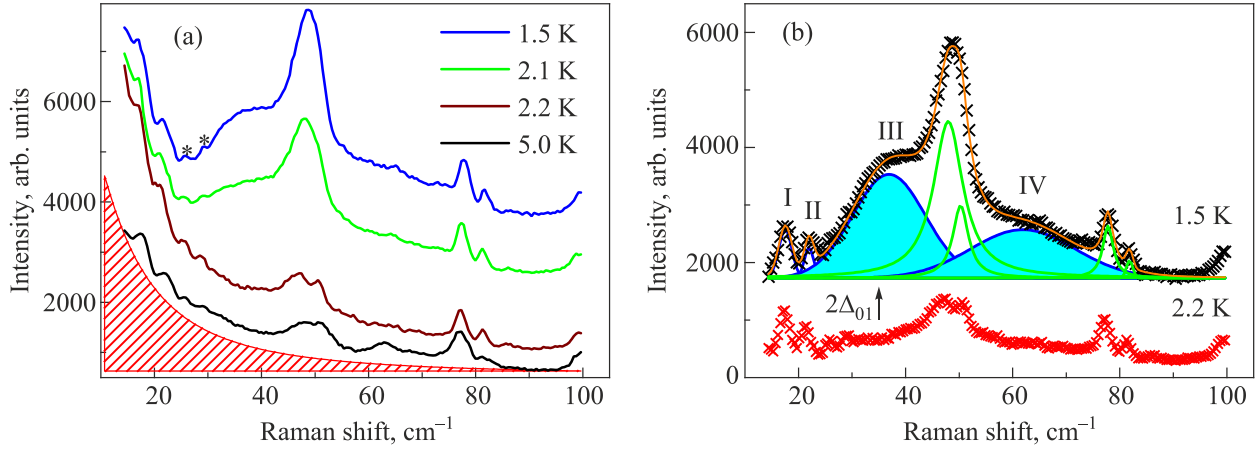


Fig. 8. (Color online) (a) Low-frequency, low-temperature Raman spectra of (CuCl)LaNb<sub>2</sub>O<sub>7</sub> at selected temperatures. Shaded area corresponds to quasielastic signal at  $T = 5$  K. Shoulders with energies  $\sim 26$  and  $\sim 28$  cm<sup>-1</sup> are marked with asterisks. (b) Fit of the spectrum at  $T = 1.5$  K by lines of phonon (green) and magnetic (blue) origin. Quasielastic signal is subtracted from the raw spectrum for clarity. The spectrum at  $T = 2.2$  K is shown for comparison.

quasiparticles as the Kitaev model may also show sharp features within the spin liquid phase.

We turn now to the distinct features found at low temperatures and energies. As Fig. 8 display, four main low-frequency maxima of magnetic origin (marked as I, II, III, and IV) with energies  $E^I = 17.5$  cm<sup>-1</sup> (2.16 meV),  $E^{II} = 21.9$  cm<sup>-1</sup> (2.7 meV),  $E^{III} = 36.9$  cm<sup>-1</sup> (4.58 meV), and  $E^{IV} = 61.9$  cm<sup>-1</sup> (7.67 meV) (at  $T = 1.5$  K) are clearly seen in the temperature range of  $T < 5$  K  $\ll \Delta$ . In addition, two weak intensity shoulders with energies  $\sim 26$  and  $\sim 28$  cm<sup>-1</sup> marked with asterisks in Fig. 8(a) are observed in the spectra. We believe that the excitation I at 17.5 cm<sup>-1</sup> is a single triplet excitation. In inelastic neutron scattering, there exist magnetic excitations at 2.31 meV (18.36 cm<sup>-1</sup>) [5] or 2.22 meV (17.9 cm<sup>-1</sup>) [18] and are attributed to the excitation of a single triplet from the singlet ground state. The single triplet branch has a very small dispersion ( $\Delta E < 0.2$  meV) pointing to extremely localized excitations [5].

In low-dimensional spin systems with strong triplet-triplet interactions (which can be caused by competing interactions and/or spin-phonon coupling), well-defined modes can appear below the magnetic scattering continuum [42–44]. These modes may be due to two triplets coupled by  $J_t$ . In this case, one expects a separation of two-particle triplet transition into three energy levels: at  $E_0 = 2\Delta - 2J_t$  for the singlet state,  $E_1 = 2\Delta - J_t$  for the triplet state, and  $E_2 = 2\Delta + J_t$  for the quintet state. Such bound states composed of two elementary triplets have been observed earlier in the low-temperature dimerized phases of CuGeO<sub>3</sub>, NaV<sub>2</sub>O<sub>5</sub>, and SrCu<sub>2</sub>(BO<sub>3</sub>)<sub>2</sub> [45–48]. Mode II at 21.9 cm<sup>-1</sup> with a linewidth comparable to mode I is certainly a lowest two-particle singlet mode. Frustration due to the interdimer coupling with magnitude  $J_{1a(2a)}/J_4$  of about  $-0.38$  in (CuCl)LaNb<sub>2</sub>O<sub>7</sub> (see notations in the Ref. 18) leads to the ratio  $E^{II} / \Delta = 1.25$ ,

matches exactly with the value of 1.25 for the case of SrCu<sub>2</sub>(BO<sub>3</sub>)<sub>2</sub> [48].

Note here that the strong temperature dependence of integrated phonon intensity of two phonon lines located on top of the magnetic response (46.7 and 50.7 cm<sup>-1</sup> at  $T = 5$  K, see Fig. 8) is consistent with the coupled dynamics of spin and phonon degrees of freedom in (CuCl)LaNb<sub>2</sub>O<sub>7</sub>.

A more complex pattern of interdimer exchange couplings, involving several non-neglected coupling constants (see Fig. 9), lead to creation several two-particle singlet modes below two-particle continuum with different energies [48–51]. Taking this into account and the proposed complex

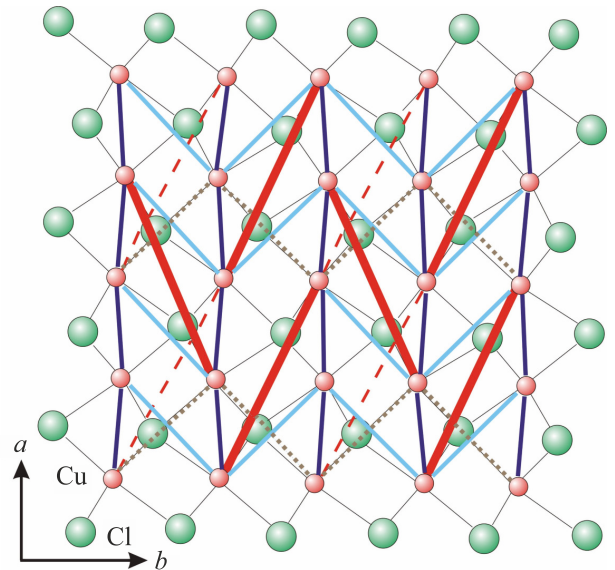


Fig. 9. (Color online) Exchange interactions in the  $ab$  plane of (CuCl)LaNb<sub>2</sub>O<sub>7</sub> [18]. Blue, solid cyan, dotted grey, solid red (strongest), and dashed red lines represent different Cu–Cu exchange interactions.

picture of exchange interactions in  $(\text{CuCl})\text{LaNb}_2\text{O}_7$  [17, 18], it can be argued that shoulders with energies  $\sim 26$  and  $\sim 28 \text{ cm}^{-1}$  can be assigned to magnetic bound states.

We now discuss the broader mode III with a FWHM =  $16 \text{ cm}^{-1}$  and center of gravity near  $36.9 \text{ cm}^{-1}$  ( $4.58 \text{ meV}$ ), slightly above twice the triplet excitation gap  $\Delta_{01} = 2.16 \text{ meV}$ . Note that the temperature behavior of mode III is identical to that of modes I and II. In neutron scattering study [5], on excitation with an energy  $5.0 \text{ meV}$  was observed and associated with a collective bound state excitation of several elementary triplets. We also tend to interpret the wide band III within the framework of correlated three triplets or more.

As to the excitation IV which appears in Raman spectra at  $61.9 \text{ cm}^{-1}$  with FWHM =  $22.8 \text{ cm}^{-1}$  and with a low-frequency cutoff at  $2\Delta_{01} \sim 35 \text{ cm}^{-1}$ , it is more appropriate to interpret it as a two-magnon continuum. The temperature behavior of the two-magnon response (not shown here) differs from that of other magnetic modes: it is retained in the spectra up to much higher temperatures due to short-range correlations [52].

It would be important to point out that all magnetic modes observed in the Raman experiment decrease their intensity for temperatures above  $5 \text{ K}$ , which is only one fifth of the spin-gap energy. A similar anomalous effect was observed also in the Raman [48] and neutron experiments [53] on  $\text{SrCu}_2(\text{BO}_3)_2$  and was attributed to the scattering on thermally excited triplet states and to the strong spin frustration, as well as to the quantum effect of some kind in this 2D Shastry–Sutherland orthogonal spin-dimer system, respectively. In the case of  $(\text{CuCl})\text{LaNb}_2\text{O}_7$ , one should assume a significant role of dynamic quantum fluctuations in the observed temperature behavior. These fluctuations are present in the ground state of  $(\text{CuCl})\text{LaNb}_2\text{O}_7$  and for finite temperatures  $T \ll \Delta$ , as evident from the analysis of the quasielastic scattering given above. Magnetic modes experience strong damping on these quantum fluctuations, and only their lowering make magnetic modes observable in the Raman spectra.

Finally, we turn to a microscopic model of the spin-gap quantum magnet  $(\text{CuCl})\text{LaNb}_2\text{O}_7$ , taking into account our Raman data. There are two independent models with a near similar arrangement of spin dimers [17, 18]. A. Tsirlin *et al.* [17, 21] established  $(\text{CuCl})\text{LaNb}_2\text{O}_7$  as a nonfrustrated system of coupled spin dimers with predominant antiferromagnetic interactions. Contrary, C. Tassel *et al.* [18] described the spin lattice of  $(\text{CuCl})\text{LaNb}_2\text{O}_7$  as Shastry–Sutherland-type antiferromagnetic dimers that are coupled by frustrated ferromagnetic interactions. Herewith, it was noted in Ref. 17 that in studies of Ref. 18 there is no experimental evidence of the magnetic frustration that is inherent to the Shastry–Sutherland model. We hope that our Raman data, namely the observation in the spectra of magnetic bound states, will resolve these discrepancies in favor of the model of C. Tassel *et al.*, since the appearance of the collective modes reflects the presence of the strong triplet-

triplet interaction, and an important parameter concerning two triplets binding effect is spin frustration due to interdimer coupling, as given by the complex pattern of competing exchange interactions shown in Fig. 9.

#### 4. Summary

We have presented first Raman scattering data of the quasi-2D quantum spin compound  $(\text{CuCl})\text{LaNb}_2\text{O}_7$  measured in the temperature range of  $1.5\text{--}295 \text{ K}$ . The goal of the work was to derive a better understanding of the spin and lattice dynamics of this compound. In order to build a correct model for  $(\text{CuCl})\text{LaNb}_2\text{O}_7$ , there are three main features to consider. The first is related to a strong spin-lattice coupling manifested in the fact that (i) new phonon lines emerge and anomalous behavior of frequencies and intensities is observed at cooling in the temperature range of the dimerization onset; (ii) there is the puzzling temperature dependence of the intensities of two phonon low-frequency lines located directly on top of the multiparticle magnetic response.

The second feature is the pronounced temperature behavior of the quasielastic scattering. It shows a plateau in the intermediate temperature range and increases with cooling up to  $T = 2.2 \text{ K}$ . This behavior indicates the presence of sizable quantum fluctuations in the system, which are possible due to the proximity to the quantum critical point that separates the singlet and long-range-ordered magnetic ground states.

Finally, we have shown that the low-energy excitation spectrum of the 2D compound  $(\text{CuCl})\text{LaNb}_2\text{O}_7$  has a rich and complex structure. At low temperatures ( $T \ll \Delta$ ), the spectra contain a one-triplet mode, several singlet modes, which are interpreted as collective two-particle singlet bound states of strongly localized triplets, a well pronounced wide band which may be interpreted within the framework of correlated three triplets, and two-magnon excitations. Importantly, geometrical frustration can play a crucial role in making the one-triplet excitation extremely localized, as noted in Ref. 5. We suppose that the drastic changes observed in the low-frequency part of the spectra at the temperature  $T = 2.1 \text{ K}$  are associated with a decrease in dynamical quantum fluctuations in the ground state of  $(\text{CuCl})\text{LaNb}_2\text{O}_7$ .

We hope that our Raman studies of  $(\text{CuCl})\text{LaNb}_2\text{O}_7$  will complete and clarify the already available information, and we want to emphasize that our observations are in favor of a model of Ref. 18 that identifies the title compound as a Shastry–Sutherland-type system with ferromagnetic interdimer couplings.

#### Acknowledgments

We acknowledge W. Brenig and J. Knolle for important discussions. This research was funded by the DFG Excellence Cluster QuantumFrontiers, EXC 2123–390837967, as well as by DFG Le967/16-1 and DFG-RTG 1952/1.

1. U. Schollwöck, J. Richter, B. J. J. Farrell, and R. F. Bishop, *Lecture Notes in Physics*, Vol. 645, Springer-Verlag, Berlin, Heidelberg (2004), p. 433.
2. J. Knolle and R. Moessner, *Annu. Rev. Condens. Matter Phys.* **10**, 451 (2019).
3. S. Sachdev, *Quantum Phase Transitions*, Cambridge University Press, Cambridge (2011).
4. T. A. Kodenkandath, J. N. Lalena, W. L. Zhou, E. E. Carpenter, C. Sangregorio, A. U. Falster, W. B. Simmons, Jr., C. J. O'Connor, and J. B. Wiley, *J. Am. Chem. Soc.* **121**, 10743 (1999).
5. H. Kageyama, T. Kitano, N. Oba, M. Nishi, S. Nagai, K. Hirota, L. Viciu, J. B. Wiley, J. Yasuda, Y. Baba, Y. Ajiro, and K. Yoshimura, *J. Phys. Soc. Jpn.* **74**, 1702 (2005).
6. K. Totsuka, Y. Narumi, M. Hagiwara, K. Kindo, Y. Baba, N. Oba, Y. Ajiro, and K. Yoshimura, *J. Phys. Soc. Jpn.* **74**, 3155 (2005).
7. A. Kitada, Z. Hiroi, Y. Tsujimoto, T. Kitano, H. Kageyama, Y. Ajiro, and K. Yoshimura, *J. Phys. Soc. Jpn.* **76**, 093706 (2007).
8. M. Yoshida, N. Ogata, M. Takigawa, J.-I. Yamaura, M. Ichihara, T. Kitano, H. Kageyama, Y. Ajiro, and K. Yoshimura, *J. Phys. Soc. Jpn.* **76**, 104703 (2007).
9. N. Oba, H. Kageyama, T. Kitano, J. Yasuda, K. Totsuka, Y. Baba, M. Nishi, K. Hirota, Y. Narumi, M. Hagiwara, K. Kindo, T. Saito, Y. Ajiro, and K. Yoshimura, *J. Phys. Soc. Jpn.* **75**, 113601 (2006).
10. M. Yoshida, N. Ogata, M. Takigawa, T. Kitano, H. Kageyama, Y. Ajiro, and K. Yoshimura, *J. Phys. Soc. Jpn.* **77**, 104705 (2008).
11. A. Kitada, Y. Tsujimoto, H. Kageyama, Y. Ajiro, M. Nishi, Y. Narumi, K. Kindo, M. Ichihara, Y. Ueda, Y. J. Uemuram, and K. Yoshimura, *Phys. Rev. B* **80**, 174409 (2009).
12. M.-H. Whangbo and D. Dai, *Inorg. Chem.* **45**, 6227 (2006).
13. A. A. Tsirlin and H. Rosner, *Phys. Rev. B* **79**, 214416 (2009).
14. Y. J. Uemura, A. A. Aczel, Y. Ajiro, J. P. Carlo, T. Goko, D. A. Goldfeld, A. Kitada, G. M. Luke, G. J. MacDougall, I. G. Mihailescu, J. A. Rodriguez, P. L. Russo, Y. Tsujimoto, C. R. Wiebe, T. J. Williams, T. Yamamoto, K. Yoshimura, and H. Kageyama, *Phys. Rev. B* **80**, 174408 (2009).
15. C.-Y. Ren and C. Cheng, *Phys. Rev. B* **82**, 024404 (2010).
16. A. A. Tsirlin, A. M. Abakumov, G. Van Tendeloo, and H. Rosner, *Phys. Rev. B* **82**, 054107 (2010).
17. A. A. Tsirlin and H. Rosner, *Phys. Rev. B* **82**, 060409(R) (2010).
18. C. Tassel, J. Kang, C. Lee, O. Hernandez, Y. Qiu, W. Paulus, E. Collet, B. Lake, T. Guidi, M.-H. Whangbo, C. Ritter, H. Kageyama, and S.-H. Lee, *Phys. Rev. Lett.* **105**, 167205 (2010).
19. S. Furukawa, T. Dodds, and Y. B. Kim, *Phys. Rev. B* **84**, 054432 (2011).
20. O. J. Hernandez, C. Tassel, K. Nakano, W. Paulus, C. Ritter, E. Collet, A. Kitada, K. Yoshimura, and H. Kageyama, *Dalton Trans.* **40**, 4605 (2011).
21. A. A. Tsirlin, A. M. Abakumov, C. Ritter, and H. Rosner, *Phys. Rev. B* **86**, 064440 (2012).
22. S. Furukawa, T. Dodds, and Y. B. Kim, *Phys. Rev. B* **84**, 054432 (2011).
23. P. Lemmens, G. Güntherodt, and C. Gros, *Phys. Rep.* **375**, 1 (2003).
24. P. Lemmens and P. Millet, *Spin–Orbit–Topology, a triptych*, in: Quantum Magnetism, U. Schollwöck, J. Richter, B. J. J. Farrell, and R. F. Bishop (eds.), *Lecture Notes in Physics*, Vol. 645, Springer-Verlag, Berlin, Heidelberg (2004), p. 433.
25. G. Caruntu and T. A. Kodenkandath, *Mat. Res. Bull.* **37**, 593 (2002).
26. V. Kurnosov, V. Gnezdilov, P. Lemmens, Yu. Pashkevich, A. K. Bera, A. T. M. N. Islam, and B. Lake, *Fiz. Nizk. Temp.* **43**, 1761 (2017) [*Low Temp. Phys.* **43**, 1405 (2017)].
27. A. A. Tsirlin, A. M. Abakumov, C. Ritter, P. F. Henry, O. Janson, and H. Rosner, *Phys. Rev. B* **85**, 214427 (2012).
28. Myung-Hwan Whangbo, Hyun-Joo Koo, and Reinhard K. Kremer, *Molecules* **26**(3), 531 (2021).
29. S. Lebernegg, M. Schmitt, A. A. Tsirlin, O. Janson, and H. Rosner, *Phys. Rev. B* **87**, 155111 (2013).
30. M. Braden, B. Hennion, W. Reichardt, G. Dhalenne, and A. Revcolevschi, *Phys. Rev. Lett.* **80**, 3634 (1998).
31. S. Zherlitsyn, S. Schmidt, B. Wolf, H. Schwenk, B. Lüthi, H. Kageyama, K. Onizuka, Y. Ueda, and K. Ueda, *Phys. Rev. B* **62**, R 6097 (2000).
32. M. J. Konstantinović, J. van den Brink, Z. V. Popović, V. V. Moshchalkova, M. Isobe, and Y. Ueda, *JMMM* **272–276**, e657 (2004).
33. B. S. Shastry and B. Sutherland, *Physica B+C (Amsterdam)* **108**, 1069 (1981).
34. J. W. Halley, *Phys. Rev. Lett.* **41**, 1605 (1978).
35. B. H. Bairamov, I. P. Ipatova, and V. A. Voitenko, *Phys. Rep.* **229**, 221 (1993).
36. P. M. Richards and W. J. Brya, *Phys. Rev. B* **9**, 3044 (1974).
37. W. J. Brya and P. M. Richards, *Phys. Rev. B* **9**, 2244 (1974).
38. B. N. Narozhny, *Phys. Rev. B* **54**, 3311 (1996).
39. A. Glamazda, P. Lemmens, S.-H. Do, Y. S. Kwon, and K.-Y. Choi, *Phys. Rev. B* **95**, 174429 (2017).
40. B. Singh, M. Vogl, S. Wurmehl, S. Aswartham, B. Büchner, and P. Kumar, *Phys. Rev. Res.* **2**, 013040 (2020).
41. Y. Gallais and I. Paul, *C. R. Phys.* **17**, 113 (2016).
42. G. S. Uhrig and H. J. Schulz, *Phys. Rev. B* **54**, 9624 (1996).
43. G. Bouzerar, A. P. Kampf, and G. I. Japaridze, *Phys. Rev. B* **58**, 3117 (1998).
44. V. N. Kotov, O. P. Sushkov, and R. Eder, *Phys. Rev. B* **59**, 6266 (1999).
45. G. Els, P. H. M. van Loosdrecht, P. Lemmens, H. Vonberg, G. Güntherodt, G.S. Uhrig, O. Fujita, J. Akimitsu, G. Dhalenne, and A. Revcolevschi, *Phys. Rev. Lett.* **79**, 5138 (1997).
46. P. Lemmens, M. Fischer, G. Els, G. Güntherodt, A. S. Mishchenko, M. Weiden, R. Hauptmann, C. Geibel, and F. Steglich, *Phys. Rev. B* **58**, 14 159 (1998).
47. P. Lemmens, M. Fischer, M. Grove, G. Els, G. Güntherodt, M. Weiden, C. Geibel, and F. Steglich, *Physica B (Amsterdam)* **259–261**, 1050 (1999).
48. P. Lemmens, M. Fischer, M. Grove, and G. Güntherodt, *Phys. Rev. Lett.* **85**, 2605 (2000).

49. Y. Fukumoto, *J. Phys. Soc. Jpn.* **69**, 2755758 (2000).
  50. C. Knetter, A. Buehler, E. Mueller-Hartmann, and G. S. Uhrig, *Phys. Rev. Lett.* **85**, 3958 (2000).
  51. H. Nojiri, H. Kageyama, Y. Ueda, and M. Motokawa, *J. Phys. Soc. Jpn.* **72**, 3243 (2003).
  52. M. G. Cottam and D. J. Lockwood, *Light Scattering in Magnetic Solids*, Wiley, New York (1986).
  53. H. Kageyama, M. Nishi, N. Aso, K. Onizuka, T. Yosihama, K. Nukui, K. Kodama, K. Kakurai, and Y. Ueda, *Phys. Rev. Lett.* **84**, 5876 (2000).
- 

### Магнітні та ґраткові збудження у квазі-2D квантовій спіновій сполуці (CuCl)LaNb<sub>2</sub>O<sub>7</sub>

Vladimir Gnezdilov, Peter Lemmens, Dirk Wulferding, Atsushi Kitada, Hiroshi Kageyama

Дані фононного раманівського розсіювання квазідвовимірної квантової спінової системи (CuCl)LaNb<sub>2</sub>O<sub>7</sub> використовуються для визначення ефективної структурної моделі, яка може послужити основою для її нетрадиційних магнітних властивостей. Крім того, спостерігається багатий спектр магнітних збуджень, включаючи квазіпружні флуктуації щільності енергії та зв'язані стани з кінцевою енергією. Ці моди є ключем до розуміння (CuCl)LaNb<sub>2</sub>O<sub>7</sub> як системи з сильною взаємодією між добре локалізованими, внаслідок вираженої конкуренції магнітного обміну, триплетними збудженнями.

Ключові слова: квантові спінові системи, раманівське розсіювання, магнітні та ґраткові збудження.